ABSTRACT

PURVA PRABHU
Determination of particle size distribution for aerosol generated by Lechler's ultrasonic atomizer
(Under the direction of Professor MICHAEL R. FLYNN)

The particle size distribution of a vacuum pump oil aerosol (Inland-99) generated by an ultrasonic atomizer US 1 (Type 710.070.16.50, working frequency 100 kHz), manufactured by Lechler was measured in this study using a gravitational collection technique. Particles were collected on microscope slides that were treated with NYEBAR type Q solvent and analyzed by microscopy. The spread factor was determined to find the relationship between the flattened diameter of sampled particles and the true spherical diameter of the particles generated by the atomizer. The mean spread factor for Inland-99 vacuum pump oil drops collected on NYEBAR type Q solvent treated microscope slides was 1.31 with a standard deviation of 0.027. The particle size distribution was approximately lognormal. The mean value of the count median diameter for three repetitions was 22.88 μm with a standard deviation of 5.86 μm. Similarly, the mean of the geometric standard deviation was 1.66 with a standard deviation of 0.15.

ACKNOWLEDGEMENT

I dedicate this technical report to my parents Suryakant and Shubhalaxmi Ajgaonkar for their love, encouragement and support throughout my life. I would like to thank my other family members, particularly my in-laws Shrikant and Sunita Prabhu for giving me encouragement, independence and also understanding me.

I would like to thank my advisor, Prof. Michael Flynn for his guidance and help during my studies and research and Prof. David Leith for his various insights into my thesis and throughout my studies. I would also like to thank Prof. Parker Reist for his encouragement and support during my stay at UNC and Prof. Donald Fox for his help in my studies and for taking time for me as a reader.

Next, I would like to thank Renée Anthony for numerous discussions and help with my research and thesis, Maryanne Boundy for her comments, suggestions and help in editing my thesis. I would also like to thank Randy Goodman for helping me try out different alternative techniques to measure particle size distribution and Dr. Robert Bagnel for his help in the microscopy laboratory. Million thanks to all friends at Baity laboratory for their support and also to Jack Whaley and CL Lassiter for help in administrative matters.

Finally, and most importantly, I want to thank my husband Vimalanand for his love, care and for encouraging me to pursue higher studies.

TABLE OF CONTENTS

LIST OF TABLES

LIST OF FIGURES

1 INTRODUCTION

Production of test aerosols is an important part of aerosol science. These aerosols are required to conduct research, calibrate instruments and to develop and test air cleaning and sampling equipments. Test aerosols can be generated by the process of atomization where liquid gets disintegrated into airborne droplets. There are different types of atomizers, such as pressure atomizers, pneumatic atomizers, rotary atomizers, ultrasonic atomizers, and electrostatic atomizers. Compressed-air atomizers are types of pneumatic atomizers that are most widely used to generate aerosol. These atomizers generally produce particles with mass median diameters less than 10 μm. The vibrating-orifice aerosol generator and spinning-disk aerosol generators are another type of atomizer that can produce particles up to 100 μm (Hinds 1999). Ultrasonic atomizers can be used to generate aerosols over a wide range of sizes from a few microns up to about 150 μm (Lefebvre, 1989).

A human can inhale particles up to size of 100μm (ACGIH 2002). Thus, studies to determine the fate of the inhalable particles require the generation of aerosol over a wide range of sizes with maximum diameter up to 100 μm. One such study is being conducted in the Baity Laboratory, University of North Carolina at Chapel Hill. The purpose of this research was to generate test aerosol for the above-mentioned study and determine its particle size distribution.

As discussed above, vibrating orifice aerosol generator, spinning-disk aerosol generator and an ultrasonic atomizer can generate particles up to 100 μm. Because of functioning difficulties with a vibrating orifice aerosol generator and spinning–disk aerosol generator, an ultrasonic atomizer US 1 (Type 710.070.16.50, working frequency 100 kHz), manufactured by Lechler (St. Charles, IL) was selected to generate the test aerosol. Lechler's atomizer generates polydisperse particles with diameters ranging from 2-100 μm. The objective of this research was to determine the particle size distribution of a vacuum pump oil (Inland-99, Churchville, NY) aerosol generated by this atomizer.

1.1 Ultrasonic atomizer

"An ultrasonic atomizer generates aerosols without the use of high pressure or atomizing air. The particles leave the nozzle with no feed velocity and their fall is affected by only gravity and ambient air conditions. Air assisted units are available which have no function in the atomization but solely in assisting with control of the spray pattern" (TPS Inc., 2003). The principle of atomization for Lechler's ultrasonic atomizers is available from the manufacturer and is attached in Appendix A. Ultrasonic atomization is basically a capillary wave phenomenon. Here capillary waves are formed on the surface of a liquid on a vibrating surface. As the frequency of excitation increases, the peak of the wave is cut into a droplet. The mean size of the drops is related to the wavelength of the capillary waves. The capillary wavelength λ is given by the following equation (Mercer 1973).

$$\lambda = \left(\frac{8\pi\sigma}{\rho\omega^2} \right)^{1/3} \qquad (1)$$

where

λ = capillary wavelength
σ = surface tension, dynes/cm
ρ = density of the liquid, g/cm^3
ω = frequency of vibration, Hz

The above ultrasonic theory is supported by experimental results carried out by various scientists. One such development of capillary wave theory was given in Lefebvre (1989). It predicts mean drop size produced by ultrasonic atomization that is given by following expression.

$$D = \left(\frac{4\pi^3\sigma}{\rho_l \omega_o^2} \right)^{1/3} \qquad (2)$$

where

D = mean drop diameter, cm
σ = surface tension, dynes/cm
ρ_l = density of the liquid, g/cm^3
ω_o = frequency of vibration, radians/sec

The mean drop diameter of aerosol produced by the Lechler atomizer was compared with Equation 2.

Information about the particle size distribution for aerosols generated by the Lechler atomizer is available from the manufacturer. These data are based on atomizing water, which has density of 1 g/cm^3, viscosity of 1.0 x 10^{-2} **P**, and surface tension of 72.7 dyne/cm under laboratory conditions. The data are summarized in Table 1. The operating liquid flow rate range is given as 1.67- 16.67 ml/min. The

manufacturer used a Phase Doppler Particle Analyzer to measure the particle size distribution of the water aerosol.

1.2 Selection of fluid

Inland-99 vacuum pump oil was selected for these studies based on its low toxicity and ease of clean up. This oil has a density of 0.86 g/cm^3, viscosity of 0.2408 P at 40 C, and a surface tension of 34 dyne/cm (Tan 2000).

The size distribution of Inland oil aerosol generated by Lechler's atomizer was expected to be different from that of water because of the physical differences between the Inland oil and water. The higher surface tension and the higher density of water is expected to result in a larger mean diameter than the oil (Equation 1).

1.3 Selection of appropriate method for measurement of particle size distribution

One of the most important factors in the selection of instrumentation for aerosol measurement is the size range of the aerosol. The atomizer produces a water aerosol with the range from 2 to 90 μm. Based on some preliminary analyses, the size range generated by the atomizer for Inland 99 vacuum pump oil was between 2 and 150 μm.

There are two general approaches to aerosol measurement: (a) direct reading instruments and (b) collection and analysis techniques.

One of the direct reading instruments is the Aerosizer (TSI, Minneapolis, MN). The Aerosizer is a "time of flight" instrument that can provide real time, high-resolution measurements over a size range of 0.5-200 μm (Tsai *et al.*, 1997). There are limitations to the use of the Aerosizer for measuring wide ranges of liquid particles. Extraction and transport of an aerosol consisting of large liquid droplets are difficult due to aspiration losses and adhesion of the particles on the inside surface of the sampling probe. After air reaches the sonic nozzle, large liquid particles may impact with the nozzle wall before exiting into the measurement region due to super-sonic conditions within the nozzle (Thornburg *et al.*, 1999). These liquid particles then stick to the nozzle wall resulting in losses. These conditions result in size measurement errors due to the removal of large particles from the sampled aerosol. In addition, particle deformation of a liquid aerosol in the sensing zone has caused underestimation of the actual aerodynamic diameter (Tsai *et al.*, 1997).

Phase Doppler Particle Analyzer (AER, TSI, Minneapolis, MN) and Particle Dynamics Analyzer (PDA, Dantec Inc., Skovlunde, Denmark) are in-situ sensing instruments that can be used to size droplets between 0.5 μm and 1.0 cm (Baron and Willeke, 2001). These instruments use phase Doppler anemometry technique, but are very expensive and were not available for use.

The cascade impactor is a collection device that is used to determine particle size distributions. The maximum cut diameter for a low-pressure impactor is 35 μm (Baron and Willeke, 2001). Therefore, it would be very difficult to quantify particle

size distributions for aerosols generated by this atomizer. Hence, this method was not selected.

Because of these problems, a gravitational collection and analysis technique was used. Particles were collected on a sampling plane in a settling chamber and analyzed by microscopy. Microscopic analysis of aerosol particles permitted accurate measurements of particle diameters.

2 METHODOLOGY

2.1 Collection of particles

Aerosol particles generated by the atomizer were collected in a vertical settling chamber of dimensions 60 cm x 60 cm x 60 cm. The top of the chamber was kept open and the ultrasonic atomizer was centrally positioned 60 cm from the bottom of the chamber, as shown in Figure 1.

To minimize the airflow in the vicinity of the experiments, the entire system was placed inside a closed wind tunnel. Prior to the beginning of each experiment, a fan was operated to generate airflow with a velocity of approximately 50 fpm for 15 minutes to purge any aerosol from the wind tunnel.

The three connections at the top of the atomizer attached to the liquid, air and power supplies. The liquid flow was controlled using a Masterflex® L/S™ computerized drive pump (Cole-Parmer, Vernon Hill, IL). The calibration for this pump is shown in Appendix B. The liquid flow rate was set at 1.84 ml/min with a standard deviation of 0.064 ml/min. Airflow was measured using a Dry Cal DC-Lite Primary flow meter (BIOS, DCL-M Rev. 1.08, Butler, NJ). Airflow was maintained at 2 lpm. The oscillator HF-power was set to the maximum.

Particles smaller than 5 μm diameter were not considered for measurement. The manufacturer's data for water indicate that particles below 5 μm account for only 0.5% of total number and 0.001% of the total mass of particles generated by the atomizer. Because of the small contribution to both mass and count, and our interest in large sized particles, particles smaller than 5 μm were not measured for our study.

The settling time of 15 minutes was selected to allow a 5 μm particle to fall 60cm, the height of the chamber. The time required for particle settling is a function of its settling velocity. Settling velocity for 5 μm particle was calculated using Equation 3.

$$V_{TS} = \frac{\rho_p d_p^2 \, g C_c}{18\mu} \qquad (3)$$

where

V_{TS} = particle settling velocity
μ = viscosity of air
g = gravitational acceleration
ρ_p = density of particle
Cc = Cunningham correction factor
d_p = diameter of particle.

The experiment was conducted as follows. The atomizer was switched on first, and was followed by the air and liquid supplies. The liquid flow was run for ten seconds, as controlled by a timer. This run time was based on the generation of a sufficient number of particles without overloading the sampling slides.

The settled particles were collected on microscope slides coated with 2% NYEBAR type Q solvent (NYE Lubricants Inc., New Bedford, MA). NYEBAR type-Q solvent is an oil retardant that minimized the spread of droplets on the slides. The coated slides were dried for 24 hours to evaporate the solvent. The slides were covered with Aluminum foil to prevent contamination by airborne particles. Eight glass microscope slides were placed at the bottom of the chamber on a circular sampling plane shown in Figure 2. The location of these sampling slides was decided as per Latin square sampling method (Feldman 1982). The circular plane area was divided into 8 concentric rings of equal area. The more the number of rings the less the radial variation of particle density within each ring. In addition, sufficient width of the ring is needed to place a microscopic slide. The maximum number of rings that can be fitted into a 60 cm diameter circular plane was 8. Division of this circle was then superimposed with 8 equal area sectors, resulting in 64 equal area regions. A sector was randomly selected from each of these concentric rings, excluding sectors that were already selected. A slide was placed in the middle of each selected sector. Thus, each ring was sampled once and each sector was sampled once and their combination was random. Thus, the total number of slides in each experiment was 8. The slides were oriented with the short axis along the radius of the circle. To improve the precision of results, these tests were performed three times.

2.2 Measurement of particle size distribution

Slides were collected and analyzed on the same day using a Nikon Microphot-FXA microscope (280X) fitted with a camera arrangement. The camera fed pictures

to a computer. Spatial calibration was made using automatic image processing software, NIH Image (Research Services Branch, 2003), and a stage micrometer. Twenty fields were selected randomly and examined along the centerline of each slide. The total number of particles from each experiment ranged from 1377 to 2748.

NIH Image software was used to analyze the pictures. Images were enhanced by using the density slice function. The diameter of each drop in the image field was then measured. Particles touching edges were ignored in the analysis.

The flattened diameter of sampled particles was converted to the actual spherical drop diameter by using the measured spread factor for Inland-99 oil. Measurement of spread factor is presented in the next section. Data were aggregated for each experiment to determine the size distribution generated by the atomizer.

2.3 Measurement of the spread factor

Additional tests were conducted to determine the spread factor. Even with the use of the oil spread retardant, droplets tended to flatten on the glass slides due to interfacial forces. Therefore, the droplet diameter observed on the slide was greater than the diameter of the original airborne droplet. The ratio of the apparent droplet diameter, d_o, as measured on a microscope slide, to the true diameter of a spherical drop, d_p, is defined as the spread factor, β:

$$\beta = \frac{d_o}{d_p} \tag{4}$$

For these tests, droplets generated by the atomizer were collected on microscope slides coated with NYEBAR type-Q solvent. Precautions were taken to avoid overloading of particles. The side views of the drops were taken with a Wild Macro Scope fitted with a camera (magnification 100X-140X). The slides were balanced on their edge and supported by a block in the viewing area of the Macro Scope. Photographs were taken of the particles that deposited near the slide's edge, and the stage micrometer was placed in the same focal plane as the drops for calibration. These photographs were taken within a period of two hours of sampling. Images of these drops were also analyzed using NIH Image software. The height, h, and flattened diameter, d_o, of the drops were measured using the edge finding function. The spread factor, β, was calculated from an equation given in Olan-Figueroa (1982).

$$\beta = \frac{d_0}{\left[h\left(\frac{3}{4}\ d_o^{\,2} + h^2\right)\right]^{1/3}} \qquad (5)$$

A total of 41 drops were analyzed to determine the spread factor.

To investigate the effect of time on the spread factor, the slides loaded with oil drops were stored for 3 days under laboratory conditions and then reanalyzed. An investigation of the spread factor on treated 2.0 μm pore size Nuclepore® polycarbonate filters was also conducted.

3 RESULTS AND DISCUSSION

3.1 Analyses of the spread factor

Figure 3 and Figure 4 represent typical photographs of the side view of the oil droplets that collected on the NYEBAR treated microscope slides and polycarbonate filters, respectively. Height and flattened diameter of these drops were measured to get the spread factor.

Spread factor for slides and filters

The spread factor was measured from 41 airborne particles with sizes from 25 to 120 μm for both slides and filters. The mean value of the spread factor for Inland-99 vacuum pump oil drops collected on NYEBAR type Q solvent treated microscope slides was 1.31 with a standard deviation of 0.027. The mean value for Nuclepore® polycarbonate filters was 1.31 with a standard deviation of 0.030. A t-test indicated that the spread factor did not vary with the sample collection media ($p = 0.83$).

Other research indicates this spread factor is likely to be the same for particles smaller than what we could measure. Liu and Pui (1982) found no apparent variation in spread factors for 2 to 50 μm oleic acid droplets (surface tension = 32.3 dyne/cm) collected on microscope slides using a similar fluorocarbon oleo phobic surfactant. Carlton and Flynn (1997) found a constant spread factor (1.34) for 3-17 μm corn oil

droplets (surface tension = 32.5 dyne/cm) collected on polycarbonate filters treated with Nyebar type K oil spread retardant. For diameters larger than 17 μm, he assumed a constant spread factor because he measured 1.35 value for 400 μm particle. Therefore, the spread factor for particles smaller than 25 μm for Inland-99 vacuum pump oil was also assumed to be 1.31.

Variation of spread factor with time

The mean value of spread factor for slides that had been stored for 3 days was 1.34 with a standard deviation of 0.027. A t-test was performed to determine if the mean value had changed over time. The test confirmed that the means were statistically different ($p < 0.001$), but the difference was small about 2.3%.

Relationship between particle diameter and spread factor

To investigate the relationship between the spherical diameter of droplets and the spread factor, regression models were developed. These tests were performed to see whether the spread factor was constant over a range of 25-120 μm. The data were analyzed using the statistical package SAS (SAS Institute Inc., Cary, NC). The regression line plots are shown in Figures 5, 6 and 7. Figure 5 and Figure 6 represent the spread factor data for the NYEBAR treated microscope slides and filters, respectively, which were analyzed the same day as sampling. Figure 7 represents the spread factor data for NYEBAR treated microscope slides that were analyzed 3 days after the sampling. In all three cases, the slopes of the lines, β_1, at a 5% confidence level were not significantly different from zero. These statistical tests indicate that the

spread factor was not a function of particle size for our test range. The results are summarized in Table 2.

3.2 Analyses of particle size distribution

Figure 8 represents a typical photograph of the vacuum pump oil droplets that collected on the NYEBAR treated microscope slides. Data from these images were aggregated for each of the three experimental runs to generate cumulative count size distributions.

Data for the three experimental runs were plotted on a log- probability plot, shown in Figure 9. Data for water aerosol as obtained from the manufacturer's manual was also included in the same graph. From the graph, it appears each set of data approximates a lognormal distribution.

The count mean diameter, count median diameter (CMD), geometric mean diameter (GMD) and geometric standard deviation (GSD) were calculated. Similarly, the GSD was also determined from the graph by using the following relationship:

$$\sigma_g = \frac{84.13\%\,\text{diameter}}{50\%\,\text{diameter}} = \frac{50\%\,\text{diameter}}{15.87\%\,\text{diameter}} \qquad (6)$$

From Table 3, it appears that the differences between the calculated GSD values and those obtained from the above relationship are less than 7%. Similarly, the

differences between CMD and GMD values are less than 7%, which indicate that the data approximate lognormal distributions.

Using Equation 2, the theoretical mean diameter for Inland-99 vacuum pump oil aerosol was calculated as 23.16 μm. The average of count mean diameter from three experimental runs was 25.12 μm with a standard deviation of 5.11 μm. Thus the experimental mean value was higher than that calculated using Equation 2. The difference may be due to variation in three experimental runs or the equation used is not directly applicable to the Lechler's atomizer.

The variation in count median diameters for the three experimental runs may be attributed to the liquid flow variation and atomizer start up variability. The small variability associated with the liquid pump operation, as evidenced by the standard deviation of 0.064 ml/min, can affect the liquid flow rate. Variation of the particle size distribution with liquid flow was not investigated. The aerosol was sampled immediately after the atomizer was turned on, and the run time was very short, *i.e.*, 10 seconds. Any sputtering of the atomizer during the start up could have affected the particle size distribution. More work is needed to address this issue. When the images were analyzed, particles touching edges were neglected. The probability of large size particles being neglected is more as compared to small particles. This may cause a bias in size distribution.

4 CONCLUSIONS

The particle size distribution of vacuum pump oil aerosol generated by Lechler's ultrasonic atomizer was measured using a gravitational technique. The spread factor was used to convert the measured diameter of flattened droplets into airborne spherical diameter. The mean value of the spread factor for Inlard-99 vacuum pump oil drops collected on both NYEBAR type Q solvent treated microscope slides and filters was 1.31. The spread factor was constant for particle diameters ranging from 25 μm to 120 μm. A significant increase of the spread factor was found when the samples were stored for 3 days relative to those analyzed the same day.

The particle size distribution of Inland-99 vacuum pump oil aerosol generated by Lechler's US-1 atomizer approximates a lognormal distribution. The mean value of the CMD was 22.88 μm with a standard deviation of 5.86 μm. Similarly, the mean of the GSD was 1.66 with a standard deviation of 0.15.

Further study is needed to minimize the variation between experiments. Future work should include the investigation of the atomizer start up issue and the effects of the liquid and the air flow rates on the particle size distribution.

5 REFERENCES

ACGIH, 2002. *Threshold Limit Values for Chemical Substances and Physical Agents & Biological Exposure Indices*, ACGIH, Cincinnati, (2002).

Baron, P. A., and Willeke, K. (2001). *Aerosol Measurement Principles, Techniques and Applications*. John Wiley & Sons, Inc. New York, p.231, 469-472.

Carlton, G. N., and Flynn M. R. (1997). Influence of spray painting parameters on breathing zone particle size distributions. *Applied Occupational and Environmental Hygiene*. 12(11): 744-750.

Feldman, H. A. Economy in sampling. Presented at the conference on the Problems of Modernization and Occupational Health, Shanghai, July, 1982.

Hinds, W. C. (1999). *Aerosol Technology, Properties, Behavior, And Measurement of Airborne Particles*. John Wiley & Sons, Inc. New York, p.432.

Lefebvre, A. H. (1989). *Atomization and sprays*. Hemisphere. New York, p.266.

Liu, B. Y. H., and Pui, D. Y. H. (1982). Drop size measurement of liquid aerosols. *Atmospheric Environment*. 16(3): 563-567.

Mercer, T. T. (1973). *Aerosol Technology in Hazard Evaluation*. Academic press. New York, p.347.

Olan-Figueroa, E., McFarland, A. R., and Ortiz, C. A. (1982). Flattening coefficients for DOP and oleic acid droplets deposited on treated glass slides. *American Industrial Hygiene Association Journal*. 43(6): 395-399.

Research Services Branch, National Institute of Mental Health, National Institute of Neurological Disorders and Stroke. http://rsb.info.nih.gov, (accessed April 02, 2003), path: NIH Image/ImageJ.

Tan, Y. (2000). The impact of transfer efficiency on worker exposure during spray painting. Ph.D. thesis. University of North Carolina at Chapel Hill, Chapel Hill, NC.

Thornberg, J., Cooper, S. J., and Leith, L. (1999). Counting efficiency of the API Aerosizer. *Journal of Aerosol Science*. 30:479-488.

TPS Inc. Fluid products. http://www.fluidproducts.com, (accessed March 21, 2003), path: Nozzles/Ultrasonic Nozzles.

Tsai, C. J., Chein, H. M., Chang, S. T., and Kuo, J. Y. (1997). Performance evaluation of an API Aerosizer™. *Journal of Aerosol Science*. 29:839-853.

Table 1. Size distribution parameters of aerosolized water for Lechler's atomizer

Ultrasonic atomizer	Operating frequency (kHz)	Count median diameter (μm)	Geometric standard deviation	Mean diameter (μm)	
		Manufacturer's data	Manufacturer's data	Manufacturer's data	Eq (2)
US 1 -Type 710.070.16.50	100	24.35	1.62	25.62	28.37

Table 2. Statistical analysis results for regression between spread factor and droplet diameter: Spread Factor = $\beta_0 + \beta_1$* Diameter

Case #	β_1	p-value	R^2
Slides analyzed same day	0.000300	0.1009	0.0675
Filters analyzed same day	0.000075	0.7205	0.0033
Slides analyzed after 3 days	0.000370	0.0872	0.0732

Table 3. Size distribution parameters of the aerosol produced by the ultrasonic atomizer.

	CMD, d_{50} μm	GMD, d_g μm (from calculation)	GSD, σ_g (From graph)				GSD, σ_g (from calculation)
			$d_{50}/d_{15.87}$	$d_{84.13}/d_{50}$	Avg	$(d_{84.13}/d_{15.87})$	
Experiment 1	29.03	27.73	1.58	1.40	1.49	1.49	1.59
Experiment 2	22.26	21.21	1.79	1.60	1.70	1.69	1.73
Experiment 3	17.36	17.13	1.83	1.74	1.79	1.78	1.78
Manufacturer's data (water)	24.35	22.82	1.68	1.53	1.61	1.60	1.67

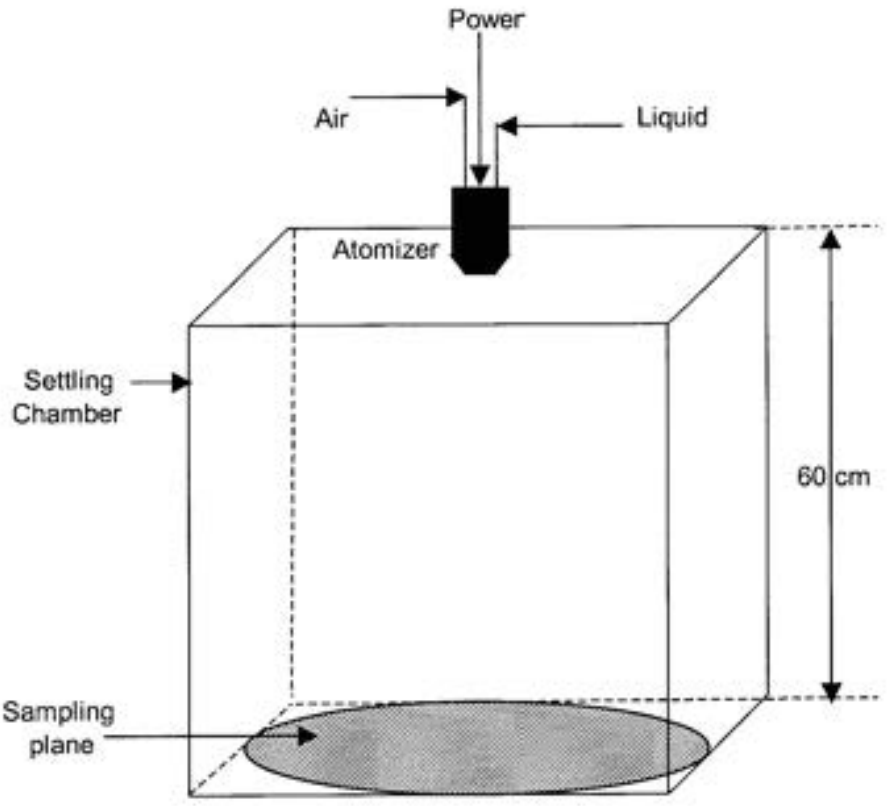

Figure 1. Schematic view of the experimental apparatus.

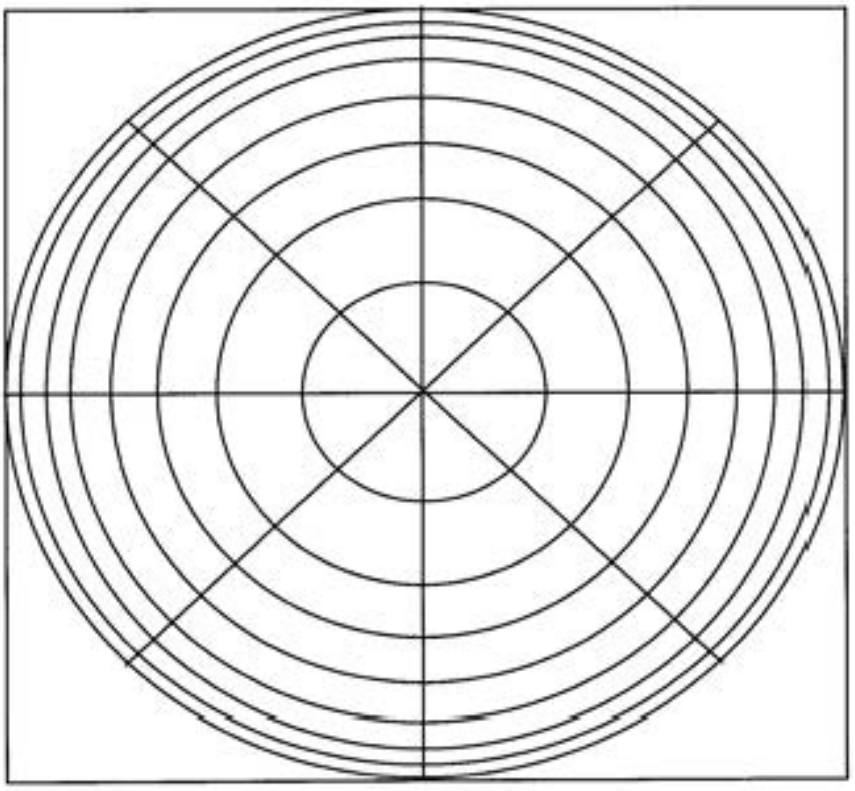

Figure 2. Latin square sampling plane

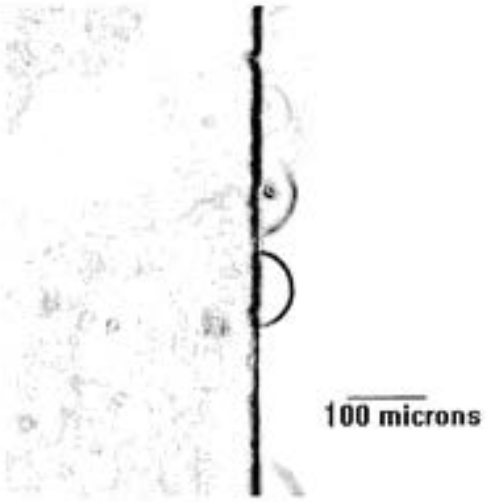

Figure 3. Side view of the oil drops collected on microscope slides viewed with Wild Macro Scope.

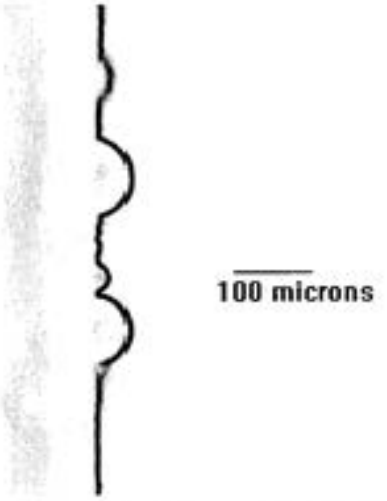

Figure 4. Side views of the oil drops collected on polycarbonate filters viewed with Wild Macro Scope.

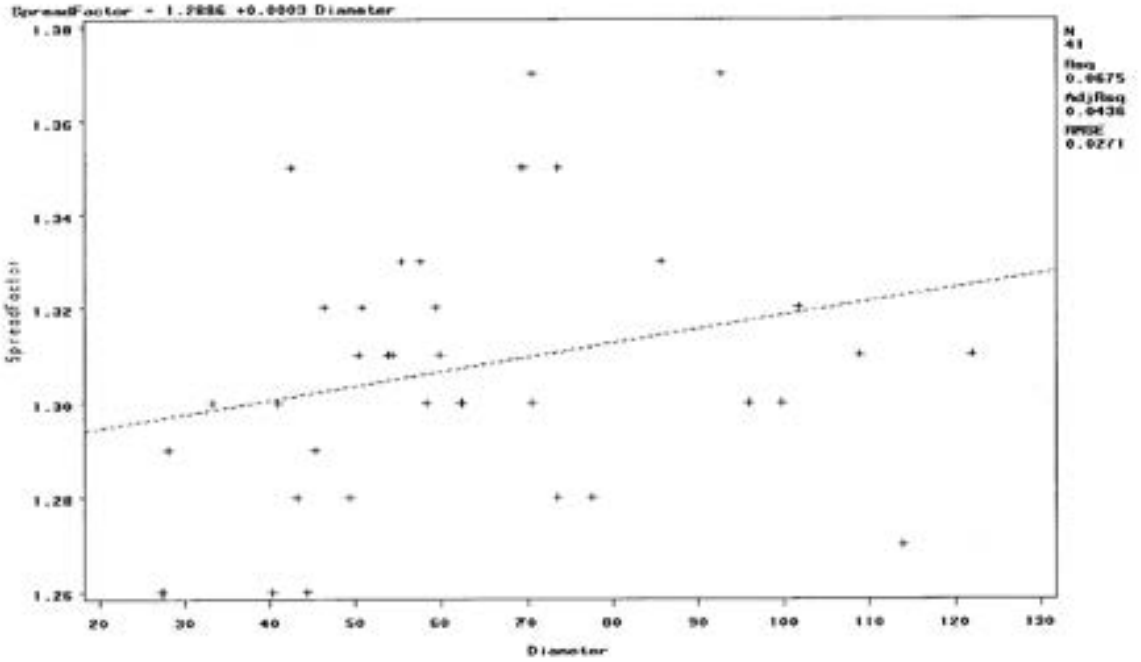

Figure 5. Regression line for spread factor of Inland-99 oil drops collected on microscope slides.

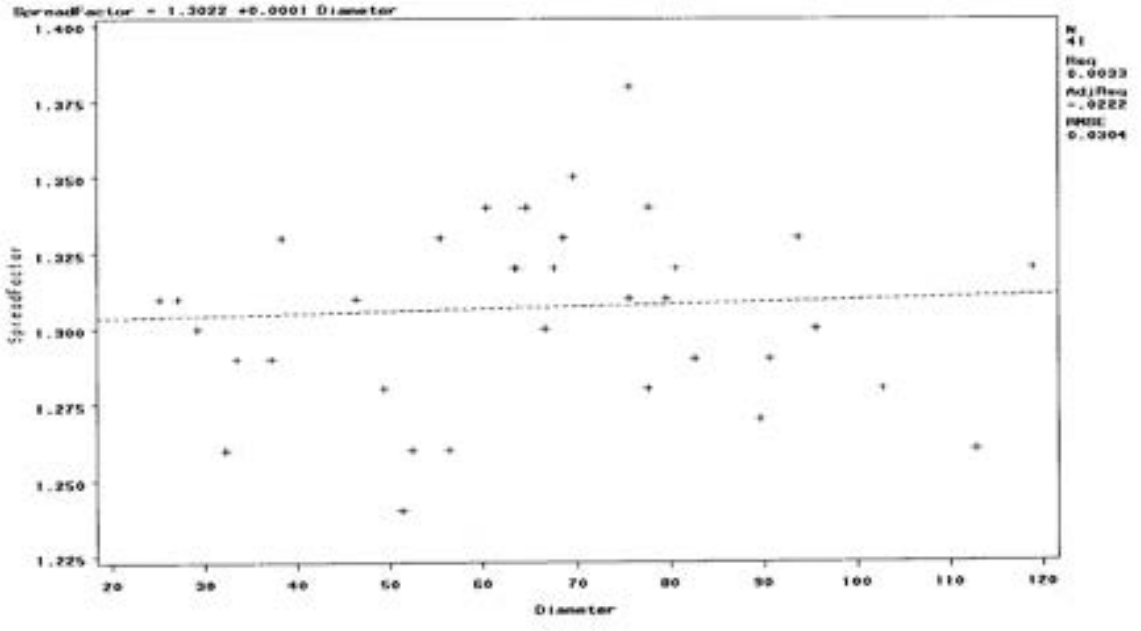

Figure 6. Regression line for spread factor of Inland-99 oil drops collected on polycarbonate filters.

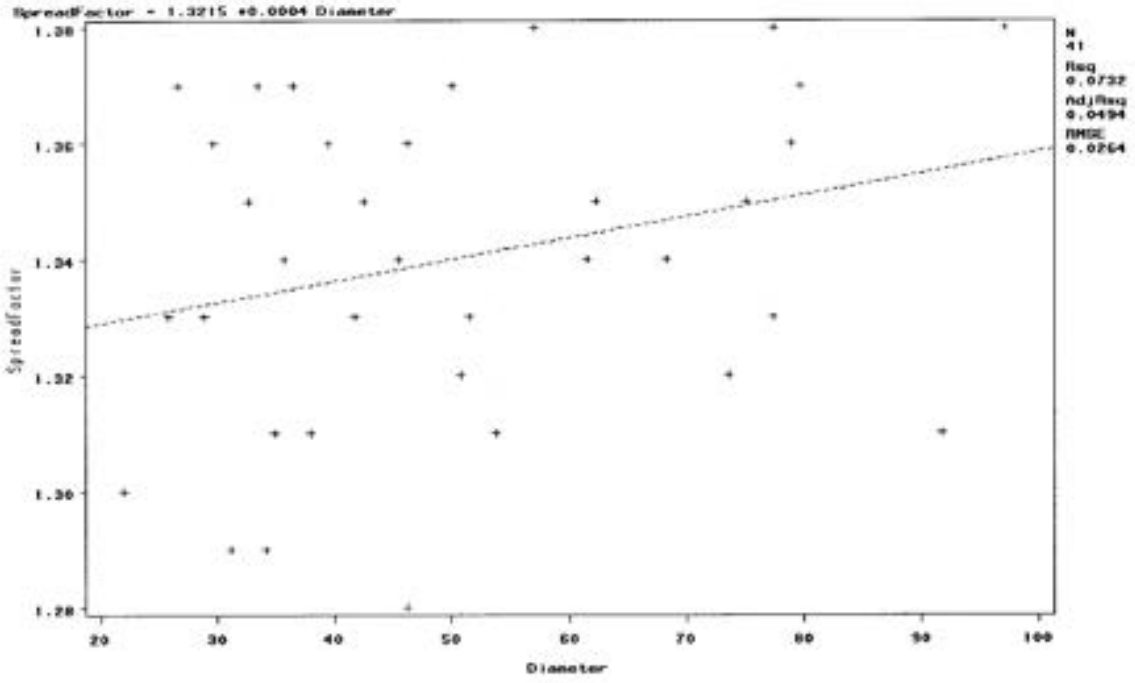

Figure 7. Regression line for spread factor of Inland-99 oil drops that were analyzed 3 days after the sample collection on microscope slides.

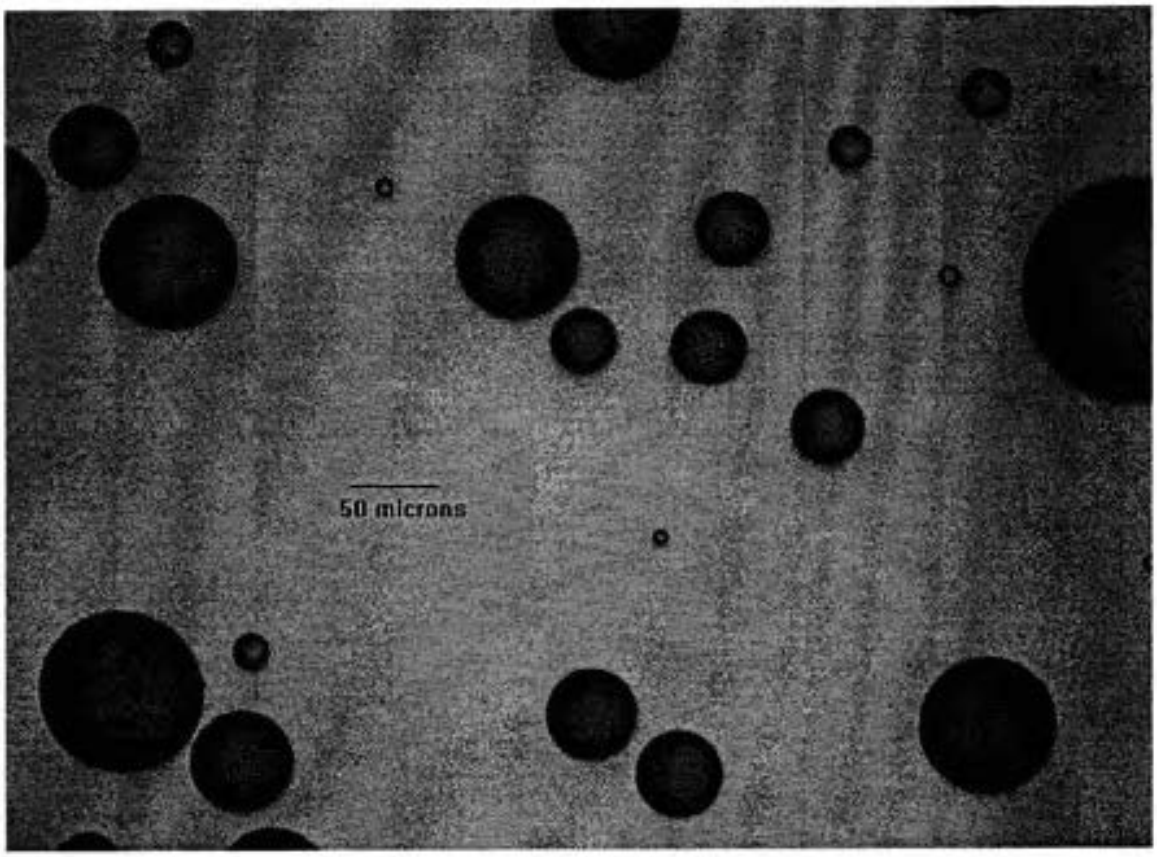

Figure 8. Oil droplets collected on treated microscope glass slides viewed with Nikon Microphot-FXA microscope

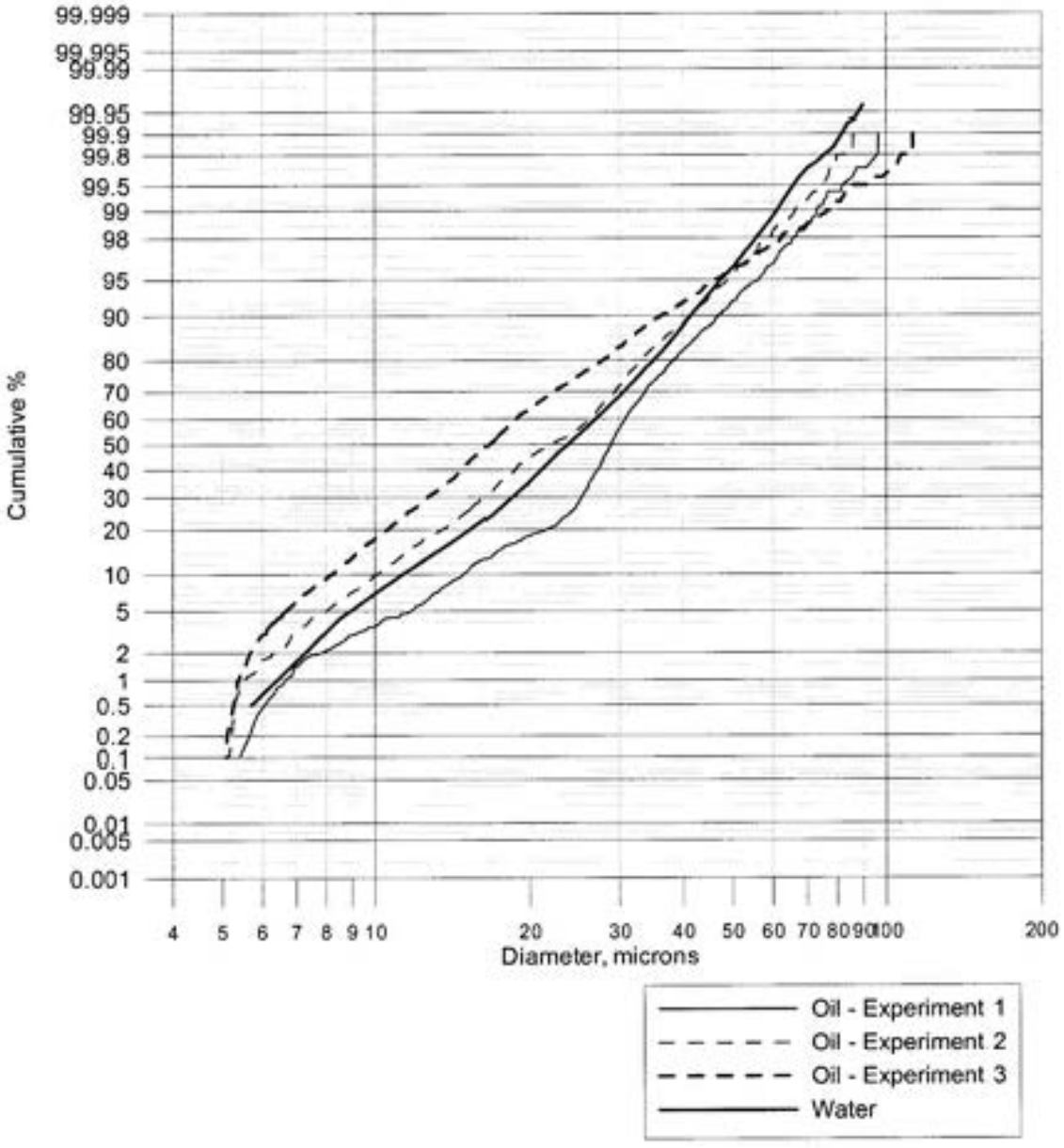

Figure 9. Cumulative count distribution for aerosol produced by the Lechler's ultrasonic atomizer.

6 APPENDIX A: PRINCIPLES OF ULTRASONIC ATOMIZER

The following paragraph, written by Lothar Bendig of Lechler, GmbH, briefly describes the principles of ultrasonic atomizers (TPS Inc., 2003).

"The atomization of liquids with Lechler's ultrasonic nozzles is based on the effect of producing capillary waves on the surface of a liquid on a vibrating surface. Contrary to gravitational waves, like in the oceans where gravity causes the restoring forces, in capillary waves the surface tension of the liquid is responsible for the development of waves. These special waves occur in the range of a small wavelength and a high frequency. That is why the surface tension has a significant influence on the atomization characteristic of ultrasonic nozzles. During atomization, capillary waves are transformed into droplets by increasing the amplitude until the peak of the wave is cut into a droplet. Each of these droplets then becomes part of the spray. Since the wavelength is a function of vibration frequency, the droplet size is determined by the frequency, which means that a high vibration frequency of the ultrasonic nozzle leads to fine droplets and a low frequency results in coarser droplets. The atomization process has a limited efficiency, which depends mainly on the viscosity of the liquid".

7 APPENDIX B: CALIBRATION CURVE FOR LIQUID PUMP

The Masterflex® L/S™ computerized drive pump manufactured by Cole-Parmer was used to supply the liquid to the atomizer. Tygon fuel and lubricant tube of size 14 was used for liquid discharge. The calibration of the pump was done using a graduated cylinder and a balance (Mettler PM34-K DeltaRange®). The calibration curve is shown in the figure below.

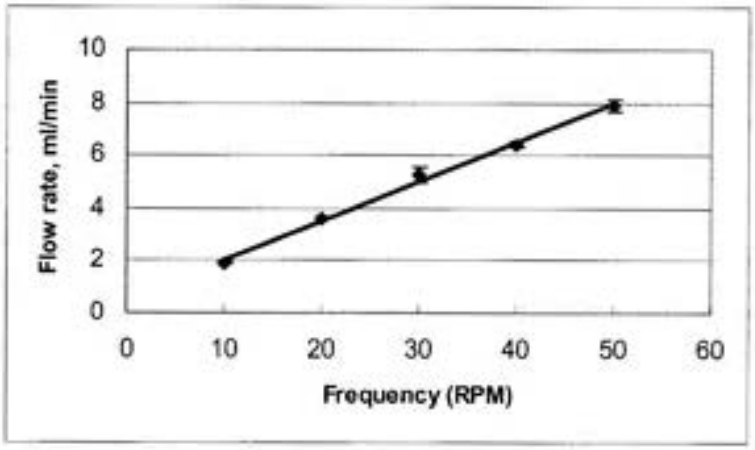

Figure 10. Calibration curve for liquid pump

After performing a regression analysis, the equation of the calibration curve was,

$$\text{Flowrate} = 0.1477 * \text{frequency} + 0.5844, \quad R^2 = 0.995$$

While conducting the experiments, the speed of rotation of the pump was 9.78 RPM, which corresponded to 2.03 ml/min according to the calibration curve. As this value of rotation was at the lower end of calibration curve, five sets of measurements at the speed of 9.78 RPM were performed. The mean value 1.84 ml/min with a standard deviation of 0.064 ml/min.

8 APPENDIX C: SPREAD FACTOR DATA

Slides analyzed same day		Slides analyzed after 3 days		Filters analyzed same day	
Spherical diameter, µm	Spread factor	Spherical diameter, µm	Spread factor	Spherical diameter, µm	Spread factor
101.68	1.32	62.21	1.35	67.48	1.32
53.92	1.31	46.29	1.36	29.21	1.30
57.68	1.33	37.93	1.31	46.33	1.31
59.94	1.31	28.83	1.33	49.32	1.28
42.49	1.35	33.38	1.37	37.26	1.29
50.83	1.32	26.56	1.37	64.46	1.34
53.87	1.31	34.90	1.31	69.49	1.35
49.37	1.28	29.59	1.36	63.47	1.32
28.08	1.29	50.83	1.32	25.18	1.31
43.25	1.28	42.49	1.35	64.46	1.34
27.40	1.26	33.38	1.37	38.29	1.33
40.90	1.30	22.00	1.30	55.41	1.33
50.85	1.32	39.45	1.36	29.21	1.30
27.32	1.26	41.73	1.33	27.12	1.31
55.39	1.33	25.80	1.33	75.52	1.35
69.49	1.35	32.63	1.35	68.50	1.33
73.53	1.28	34.14	1.29	32.23	1.26
50.38	1.31	31.13	1.29	93.71	1.33
33.24	1.30	35.66	1.34	77.66	1.34
73.52	1.35	41.73	1.33	63.59	1.32
54.39	1.31	45.54	1.34	68.50	1.33
62.45	1.30	51.60	1.33	90.66	1.29
70.51	1.30	56.89	1.38	75.54	1.31
33.24	1.30	36.43	1.37	66.54	1.30
59.42	1.32	78.90	1.36	118.88	1.32
46.35	1.32	50.07	1.37	95.69	1.30
58.43	1.30	79.66	1.37	112.81	1.26
55.39	1.33	62.21	1.35	79.58	1.31
40.29	1.26	68.28	1.34	80.57	1.32
45.33	1.29	77.38	1.38	69.49	1.35
92.64	1.37	61.47	1.34	56.40	1.26
44.34	1.26	73.61	1.32	77.57	1.28
70.51	1.37	91.81	1.31	33.39	1.29
77.55	1.28	79.66	1.37	102.74	1.28
85.67	1.33	75.11	1.35	89.64	1.27
95.87	1.30	53.88	1.31	77.55	1.28
62.52	1.30	45.53	1.34	52.37	1.26
113.86	1.27	97.11	1.38	63.47	1.32
108.79	1.31	77.39	1.33	60.43	1.34
99.71	1.30	37.95	1.31	82.60	1.29
121.92	1.31	46.28	1.28	51.36	1.24

9 APPENDIX D: STATISTICAL ANALYSIS FOR SPREAD FACTOR

Comparison of spread factor between slides and filters

t-Test: Two-Sample Assuming Equal Variances

	Variable 1	*Variable 2*
Mean	1.306357	1.307737
Variance	0.000766	0.00092
Observations	41	41
Pooled Variance	0.000843	
Hypothesized Mean Difference	0	
df	80	
t Stat	-0.21527	
P(T<=t) one-tail	0.415054	
t Critical one-tail	1.664125	
P(T<=t) two-tail	0.830107	
t Critical two-tail	1.990065	

Variation of spread factor with time

t-Test: Two-Sample Assuming Equal Variances

	Variable 1	*Variable 2*
Mean	1.306357	1.341105
Variance	0.000766	0.000715
Observations	41	41
Pooled Variance	0.000741	
Hypothesized Mean Difference	0	
df	80	
t Stat	-5.78126	
P(T<=t) one-tail	6.87E-08	
t Critical one-tail	1.664125	
P(T<=t) two-tail	1.37E-07	
t Critical two-tail	1.990065	

Relationship between particle diameter and spread factor

Slide Spread Factor – Same day analysis

The REG Procedure
Model: MODEL1
Dependent Variable: SpreadFactor

Analysis of Variance

Source	DF	Sum of Squares	Mean Square	F Value	Pr > F
Model	1	0.00207	0.00207	2.82	0.1009
Error	39	0.02858	0.00073281		
Corrected Total	40	0.03065			

Root MSE	0.02707	R-Square	0.0675
Dependent Mean	1.30707	Adj R-Sq	0.0436
Coeff Var	2.07108		

Parameter Estimates

Variable	DF	Parameter Estimate	Standard Error	t Value	Pr > |t|
Intercept	1	1.28862	0.01177	109.52	<.0001
Diameter	1	0.00029754	0.00017707	1.68	0.1009

Filter Spread Factor – Same day analysis

The REG Procedure
Model: MODEL1
Dependent Variable: SpreadFactor

Analysis of Variance

Source	DF	Sum of Squares	Mean Square	F Value	Pr > F
Model	1	0.00011967	0.00011967	0.13	0.7205
Error	39	0.03593	0.00092126		
Corrected Total	40	0.03605			

Root MSE	0.03035	R-Square	0.0033
Dependent Mean	1.30707	Adj R-Sq	-0.0222
Coeff Var	2.32215		

Parameter Estimates

Variable	DF	Parameter Estimate	Standard Error	t Value	Pr > |t|
Intercept	1	1.30218	0.01437	90.61	<.0001
Diameter	1	0.00007470	0.00020727	0.36	0.7205

Slide Spread Factor – after 3 days analysis

The REG Procedure
Model: MODEL1
Dependent Variable: SpreadFactor

Analysis of Variance

Source	DF	Sum of Squares	Mean Square	F Value	Pr > F
Model	1	0.00214	0.00214	3.08	0.0872
Error	39	0.02715	0.00069627		
Corrected Total	40	0.02930			

Root MSE	0.02639	R-Square	0.0732
Dependent Mean	1.34024	Adj R-Sq	0.0494
Coeff Var	1.96881		

Parameter Estimates

Variable	DF	Parameter Estimate	Standard Error	t Value	Pr > |t|
Intercept	1	1.32146	0.01147	115.17	<.0001
Diameter	1	0.00037080	0.00021135	1.75	0.0872